NIH Public Access
Author Manuscript
Cardiovasc Toxicol. Author manuscript; available in PMC 2011 March 1.

Published in final edited form as:
Cardiovasc Toxicol. 2010 March ; 10(1): 37–50. doi:10.1007/s12012-010-9061-3.

In Utero Exposure of Female CD-1 Mice to AZT and/or 3TC: I. Persistence of Microscopic Lesions in Cardiac Tissue

Salina M. Torres,
College of Pharmacy, University of New Mexico, Albuquerque, NM 87131, USA; Lovelace Respiratory Research Institute, Albuquerque, NM 87108, USA

Thomas H. March,
Lovelace Respiratory Research Institute, Albuquerque, NM 87108, USA

Meghan M. Carter,
Lovelace Respiratory Research Institute, Albuquerque, NM 87108, USA

Consuelo L. McCash,
Lovelace Respiratory Research Institute, Albuquerque, NM 87108, USA

Steven K. Seilkop,
SKS Consulting Services, Siler City, North Carolina 27344, USA

Miriam C. Poirier,
Center for Cancer Research, National Cancer Institute, NIH, Bethesda, MD 20892, USA

Dale M. Walker, and
BioMosaics, Inc., Burlington, VT 05405, USA

Vernon E. Walker
Lovelace Respiratory Research Institute, Albuquerque, NM 87108, USA; BioMosaics, Inc., Burlington, VT 05405, USA; Genetic Toxicology Laboratory, Department of Pathology, University of Vermont, 665 Spear St., Burlington, VT 05405, USA

Vernon E. Walker: vwalker@uvm.edu

Abstract

The current study was designed to delineate temporal changes in cardiomyocytes and mitochondria at the light and electron microscopic levels in hearts of mice exposed transplacentally to commonly used nucleoside analogs (NRTIs). Pregnant CD-1 mice were given 80 mg AZT/kg, 40 mg 3TC/kg, 80 mg AZT/kg plus 40 mg 3TC/kg, or vehicle alone during the last 7 days of gestation, and hearts from female mouse pups were examined at 13 and 26 weeks postpartum for histopathological or ultrastructural changes in cross-sections of both the ventricles and the interventricular septum. Using light microscopy and special staining techniques, transplacental exposure to AZT, 3TC, or AZT/3TC was shown to induce significant histopathological changes in myofibrils; these changes were more widespread at 13 weeks than at 26 weeks postpartum. While most light microscopic lesions resolved, some became more severe between 13 and 26 weeks postpartum. Transplacental NRTI exposure also resulted in progressive drug-specific changes in the number and ultrastructural integrity of cardiac mitochondria. These light and electron microscopic findings show that a subset of changes in cardiac mitochondria and myofibrils persisted and progressed months after transplacental exposure of an animal model to NRTIs, with combined AZT/3TC exposure yielding additive effects compared with either drug alone.

Correspondence to: Vernon E. Walker, vwalker@uvm.eduv.walker@biomosaics.com.

NIH-PA Author Manuscript
NIH-PA Author Manuscript
NIH-PA Author Manuscript

NIH-PA Author Manuscript

NIH-PA Author Manuscript

NIH-PA Author Manuscript

Keywords

AZT; 3TC; Cardiotoxicity; Electron microscopy; Histopathology; Mitochondrial pathology; PTAH stain; Transplacental exposure; Trichrome stain; Ultrastructural pathology

Introduction

Zidovudine (3′-azido-2′,3′-dideoxythymidine, AZT) and lamivudine (2′,3′-dideoxy-3′-thiacytidine, 3TC) are the nucleoside reverse transcriptase inhibitors (NRTIs) most commonly used as components in 'highly active antiretroviral therapy' (HAART) designed to inhibit viral replication in HIV-1-infected patients and to prevent vertical transmission of the virus during pregnancy [1,2]. Although NRTI-based drug combinations provide unquestionable benefits by reducing mother-to-child transmission of HIV-1 from ~25 to <2% [1–3], they may impose long-term health risks for cancer and mitochondrial disease as the uninfected children age [4–7]. AZT-based therapies have been found to cause mitochondrial damage in HIV-1-infected adults, with mitochondrial dysfunction considered a critical element in the development of AIDS- or treatment-related cardiomyopathy [8–10]. In transplacentally exposed children, the extent to which NRTIs affect mitochondria and the subsequent risk for developing cardiac abnormalities later in life remain controversial [1,2,5–7,11]. Most HAART regimens consist of two or more NRTIs plus a protease inhibitor or a non-nucleoside reverse transcriptase inhibitor; these combinations have been shown to be more effective clinically than monotherapy [1,2]. During pregnancy, the U.S. Public Health Service recommends that NRTI-based regimens be given during the last 6 months of pregnancy, intravenously during labor and delivery, and to the infant for 6 week postpartum [12]. However, studies of humans and monkeys, and in vitro systems using human cells, have shown that combined NRTI exposures, while highly effective in suppressing viral replication, work in an additive/synergistic fashion in producing toxic effects [6,13,14].

NRTI-related toxicity and host cell DNA damage may result in part from the mechanism by which they inhibit viral replication. AZT and other NRTIs are analogs of endogenous nucleosides and require intracellular bioactivation from the parent compound to their respective triphosphate moiety to suppress HIV-1 replication [15]. The major mode of action of AZT is to inhibit viral DNA synthesis through binding to HIV-1-specific reverse transcriptase and incorporation of 5′-AZT-triphosphate into proviral DNA; AZT-triphosphate lacks the 3′-OH of the deoxyribose sugar that serves as the site for the 5′ to 3′-phosphodiester bond with the proceeding nucleic acid, causing premature termination of proviral DNA synthesis [16]. This mode of action also results in the incorporation of NRTIs into host cell nuclear DNA and mitochondrial DNA (mtDNA), a phenomenon demonstrated to occur following transplacental exposure of mice, patas monkeys, rhesus monkeys, and newborn humans [17–19].

NRTI-induced alterations in mitochondrial structure and function are hypothesized to result from interference with various mechanisms involved in the normal maintenance of mitochondrial function, including (a) direct inhibition of mtDNA replication and repair via inhibition of mtDNA polymerase γ, (b) alterations in cellular metabolism affecting oxidative phosphorylation (OXPHOS) enzyme activity, and (c) mutations via incorporation of the NRTI into mtDNA, replication blockage, and generation of reactive oxygen species [8–10,20,21]. DNA polymerase γ, the only known regulating enzyme in mtDNA replication, is preferentially inhibited by NRTIs over other cellular polymerases and causes mtDNA depletion and disruption of mtDNA structure [20,21]. mtDNA depletion decreases the synthesis of proteins essential for OXPHOS enzyme activities, causing a disruption in OXPHOS function, energy loss via decreased ATP production, and subsequent increases in electron leakage from the

NIH-PA Author Manuscript

NIH-PA Author Manuscript

NIH-PA Author Manuscript

electron-transport chain leading to formation of reactive oxygen species that damage proteins, lipids, and mtDNA [9].

Although NRTI-based perinatal prophylaxis of HIV-1 is shorter than life-long treatment of HIV-1-infected patients, in utero exposure occurs during a developmentally sensitive period [22]. Thus, the effect of perinatal exposure could be significantly different from that seen in long-term treatment of HIV-1-infected patients, in which symptoms related to NRTI-induced mitochondrial damage often resolve after discontinuation of NRTI treatment [8,21]. It appears that uninfected infants in whom NRTI-based HIV-prophylaxis is completed after the first 6 weeks of life respond differently from NRTI-treated adult patients, as indicated by reports of persistent clinical symptoms and lactic acidemia related to mitochondrial dysfunction in uninfected children who received perinatal NRTIs [5,23–25]. Since NRTIs are central to HAART for reducing mother-to-child transmission of HIV-1 in well-resourced settings [1–3], it is important to determine the nature and magnitude of the long-term effects of in utero NRTI exposure as well as the mechanisms underlying the toxicities of these compounds [6–8,26–28].

Experiments in animal models of human transplacental exposure have demonstrated that NRTIs act as mitochondrial toxins with the potential to induce abnormalities in tissues with high energy demand such as the heart [6,8,28–30]. For example, using a B6C3F1 mouse model for in utero exposure to AZT or AZT/3TC, Walker and colleagues [28] found acute cardiac toxicity with ultrastructural pathology, loss of mitochondria, and altered echocardiographic measurements in newborn mice. Cardiac pathology and dysfunction persisted into adult life, as evidenced by significant dose-dependent heart enlargement, atypical mitochondria and myofibril alterations, changes in OXPHOS enzyme activity, and increased numbers of mtDNA mutations in female mice given AZT in utero compared with controls at 18 to 24 months of age.

The work reported here was planned to extend the latter studies [28] by examining persistence and progression of structural alterations in mitochondria and cardiac tissue at interim time points in the life of the mouse following in utero exposure to AZT, 3TC, or AZT/3TC at human-equivalent doses of the NRTIs. The temporal relationships between transplacental NRTI exposures, structural damage in mitochondria and cardiac tissue, and resolution of the initial damage burden was delineated via light microscopic and ultrastructural studies of hearts from female mice at 13 and 26 weeks of age following in utero exposure to AZT, 3TC, or a combination of AZT/3TC. A companion report examined the effects of AZT, 3TC, or AZT/3TC upon endpoints indicative of heart function, growth, and/or development, including assessments of alterations in mtDNA content, OXPHOS enzyme activities, mtDNA mutations, and echocardiography in the same mouse offspring [31].

Materials and Methods

Chemicals, Animals, and Exposures

AZT and 3TC were obtained from Byron Chemical (Long Island City, NY). Reagents used for tissue fixation and transmission electron microscopy (EM) were obtained from Ted Pella, Inc. (Redding, CA) and were of the highest grade available.

Date-mated female CD-1 mice were obtained from Charles River Laboratories (Wilmington, MA) and delivered to our animal facility on gestation day 10. After a 2-day acclimation period, pregnant dams were weighed, and, using a table of random numbers, were assigned to one of four groups (n = 3–7 pregnant mice/dose group) for treatments on gestation days 12 through 18 of an 18–19 day gestation period. The pregnant dams were weighed and lightly anesthetized with isofluorane and O_2 at 1L/min, and then a drug(s) or vehicle alone was given once daily

NIH-PA Author Manuscript

NIH-PA Author Manuscript

NIH-PA Author Manuscript

by gavage. Treatment groups were as follows: 80 mg AZT/kg bw, 40 mg 3TC/kg bw, or 80 mg AZT/kg plus 40 mg 3TC/kg bw for combined exposures. The compounds were dissolved in sterile PBS, which also served as the vehicle for treating control mice.

The care and housing of mice at Lovelace Respiratory Research Institute conformed to federal guidelines. All procedures using animals were approved by the Institutional Animal Care and Use Committee. Mice were housed in temperature (72 ± 4°F)- and humidity (50 ± 10%)-controlled rooms with 12-h light/12-dark cycle. Pregnant dams were individually housed in standard propylene mouse cages with sterilized bedding and nesting material. After parturition, the pups were housed with the dams until weaning. At weaning, female pups were weighed, ear tagged, and separated into cages. Offspring also were weighed at 7, 13, 22, and 26 week of age, depending upon whether they were held for 13 or 26 week postpartum. Certified rodent chow (#2025C from Harlan-Teklad, Indianapolis, IN) and filtered tap water were freely accessible to the mice. Daily monitoring of animals for health status/abnormal behavior was performed.

Euthanasia, Necropsies, and Disposition of Tissues

Male Offspring—Groups of male mouse offspring from each treatment group were euthanized by CO_2 asphyxiation on postpartum days 13, 15, or 21, and splenic and thymic lymphocytes were isolated to determine whether transplacental AZT and 3TC had additive or synergistic mutagenic effects at the *Hprt* locus. Results from these studies of male mice are reported elsewhere [14].

Female Offspring—Previous studies suggested that female offspring have greater sensitivity to mitochondrial damage subsequently leading to cardiac abnormalities following perinatal exposure to AZT, 3TC, or AZT/3TC [22,28,30]; therefore, in this study, only analyses of mitochondria from hearts of female offspring were conducted. Female mice were randomly selected for euthanasia, necropsy, and collection of tissues at 13 and 26 week postpartum. At necropsy, hearts and other tissues were collected for evaluation of mitochondrial integrity. Hearts were expunged of blood, weighed, sectioned, and stored or placed into appropriate fixatives for performing various assays [31]. Heart-to-body weight ratios for individual animals were then determined.

Light Microscopic Examination of Heart Sections

Hearts were sectioned at necropsy in a manner to obtain a transverse section containing ventricular free walls and the interventricular septum for visualization of cardiac tissue architecture at the light microscope level. Sections were preserved in a modified Karnovsky's fixative (2% paraformaldehyde and 2.5% glutaraldehyde in pH 7.2–7.4 sodium phosphate buffer) and kept at 4°C until processing. The heart sections were processed using standard procedures, and 10-μm sections of paraffin-embedded tissue were mounted on glass slides and stained with hematoxylin and eosin (H&E) for routine examination by light microscopy for histopathological changes. Two serial sections of heart from the same paraffin blocks were taken parallel to the H&E sections and were stained with either Masson's trichrome to distinguish connective tissue and muscle fibers or phosphotungstic acid-hematoxylin (PTAH) to identify muscle striations. Sections stained with Masson's trichrome were scored in a blinded fashion based on an approximation of the percentage of cardiomyocytes exhibiting pallor, a loss of normal intensity of staining, and ability to distinguish muscle fibers and cross-striations. The applied semi-quantitative scoring scheme is described in a footnote to Table 1.

Transmission Electron Microscopy of Heart Sections

Sections of hearts taken at necropsy for EM studies were preserved in a modified Karnovsky's fixative and kept at 4°C until processing. Heart sections from three to four female mice from

NIH-PA Author Manuscript

NIH-PA Author Manuscript

NIH-PA Author Manuscript

control and treatment groups at the 13- and 26-week time points were randomly selected and cut into three to four 1-mm thick sections for embedding. A previously described procedure was used for the preparation of cardiac tissue [28], with minor revisions. Briefly, portions of heart tissue were postfixed in 0.1 M osmium tetroxide buffer for 1 h, rinsed with water and dehydrated through a series of graded alcohol washes (50–100%) and then washed twice with propylene oxide. The tissues were then infiltrated with a series of graded propylene oxide and epoxy resin (Eponate 12 Resin) mixtures over the course of three 24-h periods and allowed to cure in pure epoxy resin in an oven at 60°C for 18 h. Thin sections were made with an ultramicrotome (Ultracut E, North Vale, NJ) and mounted on a 180 mesh grid. Uranyl acetate and lead citrate were used to stain the mounted thin sections that were allowed to dry and then observed with an electron microscope (H7000, Hitachi, Tokyo, Japan) operated at 75 kV.

For each mouse, a random numbers scheme was used to determine the field of view that would designate the starting point and also the other fields of view that would be photographed while an entire grid was scanned. Photographs were taken at 30,000× magnification or lower. A semi-quantitative scoring scheme was developed to grade each photomicrograph, and an average score was calculated for each mouse in each treatment group. These scores were used for statistical analyses and to calculate an average for each treatment group. The applied semi-quantitative scoring scheme is described in a footnote to Table 2.

Statistical Analyses

Statistical significance of the differences in body weights, heart weight as a percentage of body weight, degree of light microscopic or ultrastructural pathology in hearts of NRTI-treated groups versus vehicle-exposed mice, or one NRTI treatment group versus another group of AZT-, 3TC-, or AZT/3TC-exposed mice, were evaluated via two-way ANOVA and the Holm-Sidak method for multiple comparisons. The null hypothesis for each test states that there is no difference between the vehicle-exposed and individual treatment groups or between single NRTI and combined NRTI exposures. A P-value < 0.05 was considered significant.

Results

Gross Heart Weights and Light Microscopic Histopathological Findings in Heart Sections

No significant differences in body weights, heart weights, or heart-to-body weight ratios were found between vehicle-or NRTI-exposure groups at either 13 or 26 weeks of age (data not shown).

Light photomicrographs of cardiac tissue cross-sections, which were collected from mice at 13 and 26 weeks post-partum, were stained using standard H&E and special stains. Longitudinal sections of cardiac muscle photographed at higher magnification (200×) are illustrated (Figs. 1 and 2), but transverse and oblique sections were examined closely as well. H&E-stained sections of hearts from NRTI-exposed mice showed minor histological changes at 13 and 26 weeks of age (Figs. 1d, 2d, g, j) compared with vehicle-exposed mice (Figs. 1a and 2a), but the differences seen on H&E were not significant or quantifiable. When heart sections were stained with trichrome and PTAH (Figs. 1 and 2) alterations in myofibril, organization and integrity were readily apparent in NRTI-exposed mice compared with controls; however, the overall distribution of lesions was more easily quantified using trichrome as a differential stain at a lower magnification (40×, Fig. 3). Morphological changes found with differing stains in hearts of control and NRTI-treated mice at 13 and 26 weeks postpartum are described first below, followed by comparisons of the percentage of cardiomyocytes affected.

NIH-PA Author Manuscript

NIH-PA Author Manuscript

NIH-PA Author Manuscript

Heart sections from most vehicle-exposed mice at 13 weeks (Fig. 1a–c) and all vehicle-exposed mice at 26 weeks (Fig. 2a–c) consisted primarily (>98%) of tightly packed cardiomyocytes with central nuclei and muscle bundles of similar size that stained uniformly dark red with trichrome (Figs. 1b, 2b, and 3a) and uniformly dark blue with PTAH (Figs. 1c and 2c). Less than 2% of cardiomyocytes from 6/8 control mice necropsied at 13 weeks exhibited hypochromia (pallor) that appeared in trichrome-stained sections as occasional individual cells or small clusters of cells with uniform areas of pallor and less prominent myofibrils and cross-striations than adjacent muscle bundles (Fig. 2b). Areas of normal architecture and staining in the heart from one control mouse at 13 weeks of age were interspersed with several large clusters of hypo-chromatic cardiomyocytes with less prominent longitudinal fibers and cross-striations using trichrome or PTAH stains; these changes involved approximately 10% of the tissue cross-section (not shown). These latter findings in cardiac tissue sections of some 13-week-old mice but not in comparable sections from 26-week-old mice are reflected in the scores of 0.25 ± 0.39 versus 0.0, respectively (Table 1).

Histopathological changes in hearts from NRTI-exposed mice at 13 and 26 weeks included areas of increased basophilia (Figs. 1g, j, and 2d), multifocal or coalescing hypochromatic or mottled (mixed staining) areas (seen at low magnification, e.g., Fig. 3b), attenuation of myofibers (Fig. 1j), muscle bundles/branches with a glassy, hyaline appearance and near/total loss of distinct longitudinal fibers and cross-striations (Figs. 1e–k and 2f–l), and enlargement of the endomysial space with slightly increased numbers of satellite cells and/or macrophages (Figs. 1d, k, l, 2d, i, g, j–l). Muscle bundle thickness was variable; scattered clusters of cells had attenuated fascicles/branches reduced to less than twice the diameter of the centrally located nucleus compared with control cells with muscle bundles ~3-times the diameter of the nucleus (Fig. 1h, j–l). Fewer small clusters of dark-staining cells had thickened muscle bundles that had undergone hypertrophy to 5- to 6-times the diameter of the nucleus (not shown).

In general, the above morphologic changes were greatest in tissue sections from mice exposed to AZT/3TC and were more pronounced in hearts collected at 13 weeks than at 26 weeks, showing a general trend toward resolution of the light microscopic lesions. However, even though the large regions of hypochromia visible at low magnification at 13 weeks (Fig. 3) appeared to resolve by 26 weeks, higher magnification evaluations showed further deterioration of a subset of changes including multifocal attenuation or hypertrophy of muscle bundle thickness (Fig. 2k, l) and widening of focal endomysial spaces. In addition, heart sections from NRTI-exposed mice at 26 weeks showed evidence of loss of individual cardiomyocytes, including rare clusters of hypochromatic cells with pyknotic nuclei and/or myofibrils replaced by amorphous material or basophilic granules (not shown). These progressively worsening changes are noteworthy because they did not fit the general trend toward lesion resolution that was observed for the majority of lesions visible at the light microscopic level, and because their presence and progression were confirmed in the EM studies described below.

The overall impact of transplacental NRTI exposure on cardiac histology was dramatic at 13 weeks postpartum, with 75, 62.5, and 87.5% of mice exposed to 3TC, AZT, and AZT/3TC, respectively, showing effects upon >50% of the cardiomyocytes visible in cross-sections of heart tissue (e.g., Fig. 3a, b). The effects were greatest following transplacental AZT/3TC treatment, with 62.5% (5/8) of mice having hearts exhibiting 85–95% of cardiomyocytes with histological alterations and diminished trichrome staining of muscle bundles.

At 13 and 26 weeks of age, all three transplacental NRTI exposures induced significant histological damage compared to vehicle-exposed hearts (*P*-values from <0.001 to 0.039, Table 1). AZT/3TC induced significantly more damage than AZT at 13 weeks; the drug combination also induced more damage than either 3TC or AZT at 26 weeks (Table 1). No significant

NIH-PA Author Manuscript

NIH-PA Author Manuscript

NIH-PA Author Manuscript

differences were observed in damage levels induced by 3TC versus AZT at either time point. Both 3TC and AZT-exposed cardiac tissue underwent significant reductions in damage burden between 13 and 26 weeks ($P \leq 0.01$), showing that even though the resolution processes were not sufficient to restore normal/near normal cardiac structure, they were sufficient to induce a significant change in residual damage burden. However, for heart tissues exposed to AZT/3TC, a non-significant reduction in damage was observed. These findings show that the resolution processes taking place for all NRTI treatment groups between 13 and 26 weeks were not sufficient to restore normal cardiac structure, and the residual damage at 26 weeks after AZT/3TC exposure remained significantly greater than that associated with 3TC or AZT alone.

Electron Microscopic Findings in Heart Sections

Electron micrographs of vehicle-exposed mouse hearts at 13 week of age showed uniform ultrastructural cardiomyocyte architecture; mitochondria were arranged in cords between bundles of muscle fibers with clearly visible sarcomeres and distinct Z-discs and M-lines (Fig. 4a, b). Mitochondrial cristae were numerous, closely packed, and mitochondrial matrix electron density approached that of the Z-discs. Myofilaments were tightly packed, and granularity was minimal. A rare mitochondrion had loss of prominent cristae (Fig. 4a, above center), and an occasional small cluster had slightly enlarged mitochondria compared to adjacent mitochondria (Fig. 4b). EM findings in cardiac tissues of vehicle-exposed mice at 26 weeks of age were similar to those observed at 13 weeks of age, except that focal areas of mitochondria with mild size variation that was greater (Fig. 5a, b) than seen in heart sections of 13-week-old mice (Figs. 4a, 5b).

At 13 weeks postpartum, individual mitochondria in cardiac tissue from mice exposed to 3TC (Fig. 4c, d) had considerable size variation equal to or greater than that observed in other treatment groups (Fig. 4a, b, e–h). Scattered clusters of mitochondria had increased numbers of relatively small mitochondria, or, in contrast, mild to moderately enlarged mitochondria, with reduced numbers of cristae and matrix density when compared to that seen in control animals (Fig. 4c–d). As much as ~1/3 of the mitochondria in a field on average were atypical. Several photomicrographs from this exposure group contained areas with mitochondrial loss or ‘dropout’, where only a faint membrane remained as a mitochondrial residue (not shown). Sarcomere myofilaments were more loosely arranged than those of control mouse hearts and/or had a wavy appearance with focal electron lucent areas (Fig. 4c, d).

Ultrastructural changes in heart muscle from 13-week-old AZT-exposed mice involved ~1/3 of the mitochondria per field and included areas of relatively reduced numbers of mitochondria of normal size and electron density (Fig. 4e) and scattered clusters of mitochondria enlarged up to twice the size of a typical mitochondrion (Fig. 4f). These enlarged mitochondria were often irregularly shaped and had reduced numbers of cristae and matrix density with focal electron lucent areas (Fig. 4f). In scattered areas, sarcomere myofilaments were loosely arranged with focal areas of electron lucency, Z-discs had reduced electron density and irregular or curvilinear morphology, and increased numbers of medium and coarse electron dense granules were present.

An array of ultrastructural lesions was seen in 13-week-old AZT/3TC-exposed mice, with up to 50% of the mitochondria per field being atypical. Changes included a reduction in the total number of mitochondria present and an increase in sarcoplasmic space (Fig. 4g, lower cell), decreased cristae numbers and matrix electron density or increased cristae and membrane density making the (usually unapparent) double mitochondrial membrane visible, and scattered clusters composed of mildly to markedly enlarged and/or irregularly shaped mitochondria (Fig. 4h). Sarcomeres were composed of loosely to tightly packed myofilaments, with focal areas of irregular or curvilinear morphology, and Z-discs varied in density. Some cardiomyocytes contained mitochondria with normal ultrastructural morphology (Fig. 4g, uppermost cell),

NIH-PA Author Manuscript

NIH-PA Author Manuscript

NIH-PA Author Manuscript

while adjacent cells had a reduction in the total number of mitochondria present and an increase in sarcoplasmic space (Fig. 4g, lower cell). The phenomenon of finding two cells in the same photomicrograph with morphologically distinct populations of mitochondria was observed only in tissues from mice exposed to AZT/3TC.

Ultrastructural changes in hearts of 26-week-old 3TC-exposed mice were found in scattered areas occupying less than one-third of the sections and included increased numbers of moderately enlarged atypical mitochondria (Fig. 5d) with reduced numbers of prominent cristae (Figs. 5c, d) and increased matrix electron lucency (Fig. 5c). In focal areas, sarcomeres were composed of loosely arranged, non-parallel (wavy) myofilaments with loss of electron density and/or with loss of resolution of Z-lines and/or presence of curvilinear Z-lines (Fig. 5d). At 26-weeks, 3TC-exposed mouse heart tissue had fewer but more advanced lesions in mitochondria, as well as more changes in sarcomeres compared to cardiac tissue from the same exposure group evaluated at 13 weeks, but the earlier time point revealed greater numbers of mildly atypical mitochondria.

Changes in cardiac tissue at 26 weeks postpartum in mice exposed to AZT also affected less than one-third of the mitochondria and included loosely organized mitochondria and/or tightly packed enlarged mitochondria (Fig. 5e, f, respectively), with cristae that varied in number and electron density. Scattered mitochondria had increased matrix electron lucency. Sarcomeres were composed of loosely to tightly packed myofilaments, and in focal areas Z-discs had reduced electron density and/or were curvilinear. Other changes included increased sarcoplasmic spaces (Fig. 5e, f), occasional loss of continuity of myofibrils, and increased numbers of medium and coarse electron dense granules. Comparisons between vehicle-exposed heart tissues collected at 26 versus 13 weeks revealed subtle mitochondrial changes in the former; these changes included increased size variation between mitochondria and the presence of enlarged mitochondria with reduced numbers of cristae (Fig. 5a, b) compared to those seen in hearts of 13-week-old control mice (Fig. 4a, b).

Changes in hearts of 26-week-old mice exposed to AZT/3TC included clusters of significantly enlarged, severely damaged mitochondria with significantly reduced cristae numbers and reduced matrix density with focal electron lucent areas, cavitated mitochondria with or without marginated and truncated cristae, loosely arranged mitochondrial clusters with areas of mitochondrial ‘dropout’ or bizarre forms, and ‘giant mitochondria that spanned the length of 5 to 6 sarcomeres (Fig. 5j), with substantial changes in arrangement and electron density of cristae (Fig. 5g, h). Sarcomeres showed a range of changes including variations in electron density, in the compactness of myofibrils, and in the density and morphology of Z-discs. These changes involved from ~50% to, in one mouse, >90% of mitochondria (Fig. 5g–j).

At 13 and 26 weeks, the ultrastructural damage scores were significantly different for all treatment groups compared to the vehicle-exposed group (Table 2), findings similar to those observed in Table 1. In addition, at both time points the AZT/3TC treatment induced significantly more damage than either of the single treatments, which were not significantly different from each other. However, in contrast to the damage resolution observed by light microscopy between 13 and 26 weeks, results in Table 2 showed no significant change in the damage burden in mouse hearts exposed to 3TC or AZT ($P \geq 0.05$), and significant progression/deterioration during the same time period in heart tissues exposed to AZT/3TC ($P < 0.002$) (Table 2). Based upon the ultrastructural study results, the female mouse heart capacity for damage resolution was adversely affected by all three treatments, and AZT/3TC had a significantly greater deleterious effect upon this damage resolution capacity than 3TC or AZT.

NIH-PA Author Manuscript

NIH-PA Author Manuscript

NIH-PA Author Manuscript

Discussion

The current study was designed to delineate temporal changes in the structure of cardiac tissue and mitochondria at the light microscopic and ultrastructural levels following in utero exposure of female CD-1 mice to AZT, 3TC, or AZT/3TC. The results showed that in utero exposure of female mice to AZT, 3TC, or AZT/3TC induced a significant cardiac damage apparent at 13 weeks that remained significantly increased at 26 weeks, and AZT/3TC induced significantly greater burden than did 3TC or AZT alone. Significant differences in drug effects upon damage resolution capacity were observed at the both light and electron microscopic levels for single versus combined NRTI treatments, with AZT/3TC showing either modest but significant lesion resolution or significant lesion deterioration from 13 to 26 weeks postpartum.

The study design had a couple of limitations. First, since transplacental AZT-based exposures induced cardiovascular alterations in both male and female mice and rats [22,28,30], valuable sex-dependent differences in cardiotoxic effects of NRTIs might have been gained if both sexes had been assessed in the current study. The work was limited to female mice, however, due to restricted resources and the observations that females appeared more sensitive than males to cardiovascular effects following perinatal exposures of mice to AZT or AZT/3TC [22,28,30] or humans to NRTI-based combination drug therapies [32; unpublished data from Dr. Steven Lipshultz, University of Miami]. Second, the nature and range of ultrastructural changes in hearts of mice exposed to AZT alone versus 3TC alone appeared to have some distinctive features (not easily shown in a few figures) suggesting a possible difference in pathogenic mechanisms of the two NRTIs; the typical sample size for EM studies was too limited to develop a scheme for assessing these apparent morphological differences.

In the current study, subtle to marked changes in cardiac tissue were detected in NRTI-exposed female mice using standard and differential staining techniques on heart sections. These changes included multifocal areas of myofibrils within a hypochromatic heart section, suggestive of a decrease in myofibril density or disorganization of myofibrils such that the stain was not taken up as well. Importantly, hypochromatic areas were found to coexist in serial sections stained with trichrome and PTAH, indicating that these findings are not a phenomenon of a random staining effect. Attenuation of muscle bundles, either from a loss of myofibrils or thinning of the myocytes also occurred in hearts from NRTI-exposed mice, and was identified in sections using all three stains. Additionally, increases in endomysial space found in some heart sections may be indicative of a loss of damaged myocytes. Notably, the attenuation of muscle bundles and increase in endomysial space found by light microscopy were highly consistent with the thinning of muscle fibers and the approximate doubling of mitochondrial numbers found between muscle bundles by EM, particularly in AZT/3TC-exposed mice at 26 weeks of age.

Molecular changes associated with the resolution effects observed by light microscopy cannot be described because the molecular components that affect the binding of the special stains used in these studies have not been determined definitively to date. It is important to note, however, that this lack of knowledge should not be used as a basis for discounting the evidence of varying degrees of lesion resolution found in the light microscopy studies. Instead, the light and EM studies suggest that a variety of lesion resolution processes occur in mouse heart tissues exposed transplacentally to NRTIs, that some types of damage are resolved successfully while others are not, and that different NRTIs affect these processes differently.

Our observations of ultrastructural defects in cardiomyocytes of mice exposed in utero to AZT, 3TC, or AZT/3TC are consistent with the results of earlier studies in experimental models, including mice and monkeys. In adult mice (including transgenic and ‘AIDS’ mice), there was EM evidence of abnormal cardiac structure visible months after treatment with AZT, 3TC, and

NIH-PA Author Manuscript

NIH-PA Author Manuscript

NIH-PA Author Manuscript

other individual or pairs of NRTIs [33–36]. Bishop and coworkers [22] exposed CD-1 mice to AZT and 3TC during gestation, lactation, and up to postnatal day 28 and evaluated cardiomyocyte and mitochondrial ultrastructure at 4 weeks of age. Semi-quantitative evaluation revealed mitochondrial enlargement, disruption in arrangement and cristae, and spatial disorganization of mitochondria in exposed mice. Transplacental exposure of female mice to AZT or AZT/3TC produced acute toxicity and substantial loss of mitochondria in newborn mice leading to significantly enlarged hearts, containing frequent clusters of mitochondria and myofibrils with substantial abnormalities, at 18 to 24 months after birth [28]. In the current study of female mice exposed in utero to AZT, 3TC, or AZT/3TC, the greater range in EM lesions including myofibril alterations at 26 week of age were indicative of a progression of damage from what was seen at 13 week of age. Alterations in sarcomeres and myofibrils were not as pronounced as those seen in monkeys; yet, dissolution of Z-bands and myofibril breaks were observed in treatment groups of mice at 26 week of age. Exposure of mice to AZT/3TC together appeared to have an additive effect in producing mitochondrial and myofibril damage, including the frequent occurrence of remarkably large mitochondria not seen after single-drug treatments. It is uncertain whether these ‘giant’ mitochondria arose from fusion of two or more incompetent mitochondria as a compensatory mechanism to generate ATP, or whether fission was at work and the mitochondrion was in the process of being removed from the population.

In utero exposure of *Erythrocebus patas* monkeys to human-equivalent doses of AZT, 3TC, and other NRTIs alone or in combinations caused significant ultrastructural changes to mitochondria with myofibrillar loss and degradation of fetal cardiac and skeletal muscle at birth [30,37,38]. When exposures were extended to the postnatal period and cardiac tissue was examined ultrastructurally at 1 year of age (in other exposed monkeys), patas monkeys treated with AZT alone or in combination with other NRTIs were found to have clusters of damaged mitochondria with some EM lesions having resolved successfully, others retained without evidence of resolution, and others altered further suggesting progression [39]. Both male and female offsprings were examined in these monkey studies, but the samples sizes to date are too small to access potential gender differences [unpublished data, Dr. Miriam Poirier, NCI].

The findings of some lesions that resolved along with other lesions that deteriorated further over time suggest that multiple, differing processes may be involved in the response to transplacental exposure to NRTIs. At 13 week postpartum, as many as 95% of the cardiomyocytes in hearts of mice exposed in utero to AZT/3TC exhibited uniform or mottled hypochromatic areas or reduced staining with trichrome and PTAH, suggesting that the changes induced by transplacental NRTI treatment were pervasive. The significantly lower levels of residual histopathological changes at 26 week postpartum in NRTI-exposed mice showed the capacity of the mouse heart to resolve much of this damage. However, the occurrence of hypertrophy of some muscle bundles and increased attenuation of more muscle bundles, widening of the endomysial space, loss of individual cardiomyocytes, and progression of ultrastructural changes suggested that this damage resolution process, which appeared to be effective at the light microscopic level, was not able to alter the progression of some processes induced by the transplacental exposures. This conclusion is supported by echocardiography studies in the same NRTI-exposed mice; these studies demonstrated a decrease in left ventricular posterior wall thickness that progressed between 13 and 26 weeks postpartum in NRTI-exposed mice relative to vehicle-exposed mice [31]. The combined EM data from hearts of mice necropsied at birth, 4, 13, 26 week, and 18–24 months [22, 28, current work] support the hypothesis that transplacental exposure of mice to AZT and/or 3TC first causes acute mitochondrial and cardiac toxicity found at birth, then this damage largely resolves around 4 week of age and is followed by remodeling of some persistent lesions that lead to delayed, progressive cardiotoxicity.

NIH-PA Author Manuscript

NIH-PA Author Manuscript

NIH-PA Author Manuscript

Foster and Lyall [7] have noted that cumulative (mitochondrial) toxicities are becoming progressively apparent in children receiving HAART, and that, in an era of expanding treatment options, minimizing toxicities becomes an increasing possibility. Given that NRTIs are likely to remain the backbone of HAART for the near future, our findings in transplacentally exposed mice suggest that this experimental system may be a useful model for investigating chemoprevention of NRTI-induced mitochondrial toxicity and cardiotoxicity, in the manner that a rat model has been used to assess dexrazoxane-based prevention of doxorubicin-induced delayed cardiotoxicity [40]. Ever increasing data indicate that long-term monitoring and cardiac outcome studies of children receiving perinatal antiretrovirals is a necessity [7,32].

Acknowledgments

We wish to thank Mr. Steve Randock, Ms. Cynthia Herrera, and Ms. Wendy Piper (LRRI) for technical assistance in preparing figures and the manuscript. This work was supported, in part, by NIH grants R01 HL 72727 to VEW and 1 F31 HL081928 to SMT from the National Heart, Lung, and Blood Institute. The contents of this paper are solely the responsibility of the authors and do not necessarily represent the official views of the National Institutes of Health.

References

1. Watts DH. Treating HIV during pregnancy. An update on safety issues. Drug Safety 2006;29:467–490. [PubMed: 16752931]
2. Thorne C, Newell ML. Safety of agents used to prevent mother-to-child transmission of HIV: Is there any cause for concern? Drug Safety 2007;30:203–213. [PubMed: 17343429]
3. European Collaborative Study. Mother to child transmission of HIV infection in the era of highly active antiretroviral therapy. Clinical Infectious Diseases 2005;40:458–465. [PubMed: 15668871]
4. Poirier MC, Olivero OA, Walker DM, Walker VE. Perinatal genotoxicity and carcinogenicity of the anti-retroviral nucleoside analog drugs. Toxicology and Applied Pharmacology 2004;199:151–161. [PubMed: 15313587]
5. Blanche S, Tardieu M, Benhammou V, Warszawski J, Rustin P. Mitochondrial dysfunction following perinatal exposure to nucleoside analogues. AIDS 2006;20:1685–1690. [PubMed: 16931932]
6. Walker VE, Poirier MC. Foreword: Special issue on health risks of perinatal exposure to nucleoside reverse transcriptase inhibitors. Environmental and Molecular Mutagenesis 2007;48:159–165. [PubMed: 17358025]
7. Foster C, Lyall H. HIV and mitochondrial toxicity in children. Journal of Antimicrobial Chemotherapy 2008;61:8–12. [PubMed: 17999978]
8. Dagan T, Sable C, Bray J, Gerschenson M. Mitochondrial dysfunction and antiretroviral nucleoside analog toxicities: What is the evidence? Mitochondrion 2002;1:397–412. [PubMed: 16120293]
9. Lewis W. Mitochondrial dysfunction and nucleoside reverse transcriptase inhibitor therapy: Experimental clarifications and persistent clinical questions. Antiviral Research 2003;58:189–197. [PubMed: 12767466]
10. Lewis W. Cardiomyopathy, nucleoside reverse transcriptase inhibitors and mitochondria are linked through AIDS and its therapy. Mitochondrion 2004;4:141–152. [PubMed: 16120379]
11. Spector SA, Saitoh A. Mitochondrial dysfunction: Prevention of HIV-1 mother-to-infant transmission outweighs fear. AIDS 2006;20:1777–1778. [PubMed: 16931943]
12. U.S. Public Health Services. Available from: www.aisdsinfo.nih.gov/guidelines
13. Olivero OA, Fernandez JJ, Antiochos BB, Wagner JL, St Claire ME, Poirier MC. Transplacental genotoxicity of combined antiretroviral nucleoside analogue therapy in Erythrocebus patas monkeys. Journal of Acquired Immuno Deficiency Syndrome 2002;29:323–329.
14. Torres SM, Walker DM, Carter MM, Cook DL Jr, McCash CL, Cordova EM, et al. Mutagenicity of zidovudine, lamivudine, and abacavir following exposure of human lymphoblastoid cells or in utero exposure of CD-1 mice to single agents or drug combinations. Environmental and Molecular Mutagenesis 2007;48:224–238. [PubMed: 17358033]
15. Furman PA, Fyfe JA, Clair MH, Weihhold K, Rideout JL, Freeman GA, et al. Phosphorylation of 3′-azido-3′-deoxythymidine and selective interaction of the 5′triphosphate with human

NIH-PA Author Manuscript

NIH-PA Author Manuscript

NIH-PA Author Manuscript

immunodeficiency virus reverse transcriptase. Proceedings of the National Academy of Sciences of the United States of America 1986;83:8333–8337. [PubMed: 2430286]

16. Kakuda TM. Pharmacology of nucleoside and nucleotide reverse transcriptase inhibitor-induced mitochondrial toxicity. Clinical Therapeutics 2000;22:685–708. [PubMed: 10929917]
17. Olivero OA, Anderson LM, Diwan BA, Haines DC, Harbaugh SW, Moskal TJ, et al. Transplacental effects of 3′-azido-2′, 3′-dideoxythymidine (AZT): tumorigenicity in mice and genotoxicity in mice and monkeys. Journal of the National Cancer Institute 1997;89:1602–1608. [PubMed: 9362158]
18. Olivero OA, Shearer GM, Chougnet CA, Kovacs AA, Landay AL, Baker R, et al. Incorporation of zidovudine into leukocyte DNA from HIV-1-positive adults and pregnant women, and cord blood from infants exposed in utero. AIDS 1999;13:919–925. [PubMed: 10371172]
19. Poirier MC, Patterson TA, Slikker W Jr, Olivero OA. Incorporation of 3′-azido-3′-deoxythymidine (AZT) into fetal DNA, and fetal tissue distribution of drug, after infusion of pregnant late-term rhesus macaques with a human-equivalent AZT dose. Journal of Acquired Immuno Deficiency Syndrome 1999;22:477–483.
20. Lim SE, Copeland WC. Differential incorporation and removal of antiviral deoxynucleotides by human DNA polymerase gamma. The Journal of Biological Chemistry 2001;276:23616–23623. [PubMed: 11319228]
21. Brinkman K, ter Hofstede JM, Burger DM, Smeitink JAM, Koopmans PP. Adverse effects of reverse transcriptase inhibitors: Mitochondrial toxicity as common pathway. AIDS 1998;12:735–1744.
22. Bishop JB, Tani Y, Witt K, Johnson JA, Peddada S, Dunnick J, et al. Mitochondrial damage revealed by morphometric and semiquantiative analysis of mouse pup cardiomyocytes following in utero and postnatal exposure to zidovudine and lamivudine. Toxicological Sciences 2004;8:12–517.
23. Blanche S, Tardieu M, Rustin P, Slama A, Barret B, Firtion G, et al. Persistent mitochondrial dysfunction and perinatal exposure to antiretroviral nucleoside analogues. Lancet 1999;354:1084–1089. [PubMed: 10509500]
24. Alimenti A, Burdgec DR, Ogilvie GS, Money DM, Forbes JC. Lactic acidemia in human immunodeficiency virus-uninfected infants exposed to perinatal antiretroviral therapy. Pediatric Infectious Disease Journal 2003;22:782–788. [PubMed: 14506368]
25. Poirier MC, Divi RL, Al-Harthi L, Olivero OA, Nguyen V, Walker B, et al. Long-term mitochondrial toxicity in HIV-uninfected infants born to HIV-infected mothers. Journal of Acquired Immuno Deficiency Syndrome 2003;33:175–183.
26. Wutzler P, Thust R. Genetic risks of antiviral nucleoside analogues-a survey. Antiviral Research 2001;49:55–74. [PubMed: 11248359]
27. Kohler JJ, Lewis W. A brief overview of mechanisms of mitochondrial toxicity from NRTIs. Environmental and Molecular Mutagenesis 2007;48:166–172. [PubMed: 16758472]
28. Walker DM, Poirier MC, Campen MJ, Cook DL Jr, Divi RL, Nagashima K, et al. Persistence of mitochondrial toxicity in hearts of female B6C3F1 mice exposed in utero to 3′-azido-3′-deoxythymidine. Cardiovascular Toxicology 2004;4:133–153. [PubMed: 15371630]
29. Chan SS, Santos JH, Meyer JN, Mandavilli BS, Cook DL Jr, McCash CL, et al. Mitochondrial toxicity in hearts of CD-1 mice following perinatal exposure to AZT, 3TC, or AZT/3TC in combination. Environmental and Molecular Mutagenesis 2007;48:190–200. [PubMed: 16395692]
30. Divi RL, Leonard SL, Kuo MM, Nagashima K, Thamire C, St Claire MC, et al. Transplacentally exposed human and monkey newborn infants show similar evidence of nucleoside reverse transcriptase inhibitor-induced mitochondrial toxicity. Environmental and Molecular Mutagenesis 2007;47:01–20.
31. Torres SM, Divi RL, Walker DM, McCash CL, Carter MM, Campen MJ, et al. In utero exposure of female CD-1 mice to AZT and/or 3TC: II Persistence of functional alterations in cardiac tissue. Cardiovascular Toxicology. 2010 in press.
32. Lipshultz SE, Shearer WT, Rich K, Thompson B, Cheng I, Harmon T, et al. Antiretroviral therapy (ART)—associated cardiotoxicity in uninfected but ART-exposed infants born to HIV-infected women: The prospective NHLBI CHA-ART-1 study. Mutation Research-Fundamental and Molecular Mechanisms of Mutagenesis 2005;28:9.

NIH-PA Author Manuscript

NIH-PA Author Manuscript

NIH-PA Author Manuscript

33. Lewis W, Haase CP, Raidel SM, Russ RB, Sutliff RL, Hoit BD, et al. Combined antiretroviral therapy causes cardiomyopathy and elevates plasma lactate in transgenic AIDS mice. Laboratory Investigation 2001;81:1527–1536. [PubMed: 11706060]

34. Szabados E, Fischerc GM, Toth K, Csetev B, Nemeti B, Trombitas K, et al. Role of reactive oxygen species and poly-ADP-ribose polymerase in the development of AZT-induced cardiomyopathy in rat. Free Radical Biology and Medicine 1999;26:309–317. [PubMed: 9895221]

35. Lewis W, Grupp I, Grupp G, Hoit B, Morris R, Samarel AM, et al. Cardiac dysfunction occurs in the HIV-1 transgenic mouse treated with zidovudine. Laboratory Investigation 2000;80:187–197. [PubMed: 10701688]

36. Lewis W, Haase CP, Miller YK, Ferguson B, Stuart T, Ludaway T, et al. Transgenic expression of the deoxy-nucleotide carrier causes mitochondrial damage that is enhanced by NRTIs for AIDS. Laboratory Investigation 2005;85:972–981. [PubMed: 15951836]

37. Gerschenson M, Erhart SW, Paik CY, St Claire MC, Nagashima K, Skopets B, et al. Fetal mitochondrial heart and skeletal muscle damage in Erythrocebus patas monkeys exposed in utero to 3′-azido-3′-deoxythymidine. AIDS Research and Human Retroviruses 2000;16:635–644. [PubMed: 10791874]

38. Gerschenson M, Nguyen V, Ewings EL, Ceresa A, Shaw JA, St Claire MC, et al. Mitochondrial toxicity in fetal Erythrocebus patas monkeys exposed transplacentally to zidovudine plus lamivudine. AIDS Research and Human Retroviruses 2004;20:91–100. [PubMed: 15000702]

39. Divi RL, Leonard SL, Kuo MM, Walker BL, Orozco CC, St Claire MC, et al. Cardiac mitochondrial compromise in 1-yr-old Erythrocebus patas monkeys perinatally-exposed to nucleoside reverse transcriptase inhibitors. Cardiovascular Toxicology 2005;5:333–346. [PubMed: 16244378]

40. Lebrecht D, Geist A, Ketelsen UP, Haberstroh J, Setzer B, Walker UA. Dexrazoxane prevents doxorubicin-induced long-term cardiotoxicity and protects myocardial mitochondria from genetic and functional lesions in rats. British Journal of Pharmacology 2007;51:771–778. [PubMed: 17519947]

Abbreviations

AZT	Zidovudine or 3′-azido-2′, 3′-dideoxythymidine
EM	Transmission electron microscopy
H&E	Hematoxylin and eosin
HAART	Highly active antiretroviral therapy
mtDNA	Mitochondrial DNA
NRTIs	Nucleoside reverse transcriptase inhibitors
OXPHOS	Oxidative phosphorylation
PTAH	Phosphotungstic acid-hematoxylin
3TC	Lamivudine or 2′,3′-dideoxy-3′-thiacytidine

NIH-PA Author Manuscript
NIH-PA Author Manuscript
NIH-PA Author Manuscript

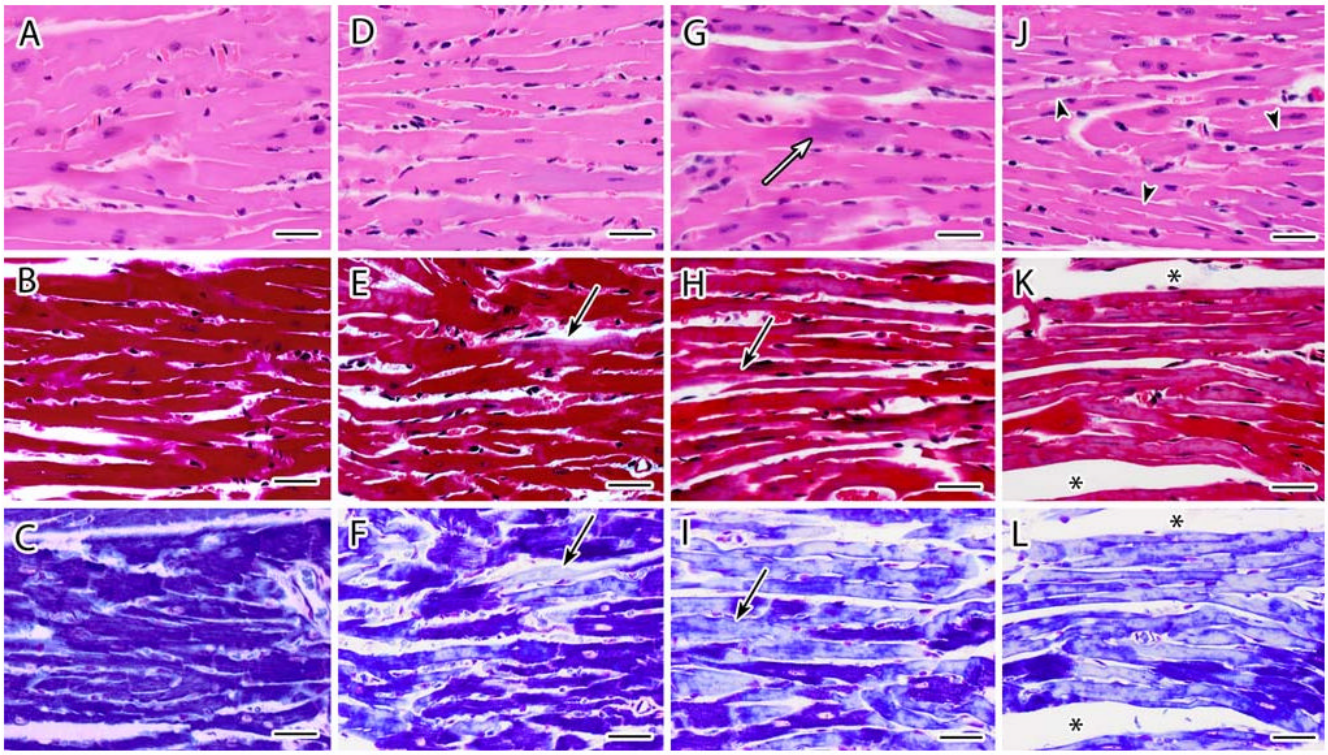

Fig. 1.

a–l Representative light photomicrographs of cardiac tissue sections stained with H&E (*top panel*), Masson's trichrome (*center panel*), and PTAH (*lower panel*) from female CD-1 mice necropsied at 13 week of age following transplacental exposure to vehicle (**a, b, c**), 3TC (**d, e, f**), AZT (**g, h, i**) or AZT/3TC (**j, k, l**) on days 12–18 of gestation. Heart sections from vehicle-exposed mice demonstrate characteristic features of cardiomyocytes with H&E (**a**) and uniform dark staining of myofibrils with trichrome and PTAH (**b, c**). An increase in basophilic staining (*white arrow*) and an attenuation of myofibers (*arrowhead*) was visualized with H&E staining in heart sections from NRTI-exposed mice (**g,j**). For trichrome and (**e, h, k**) and PTAH (**f, i, l**) staining, NRTI exposure resulted in pale or mottled (mixed staining) muscle bundles with some areas having a hyaline appearance with loss of distinct fibers and cross-striations (*black arrows*). Increases in endomysial space were seen most often in AZT/3TC-exposed mice (*asterisks*). Photomicrographs from each group represent parallel and serial sections from the same paraffin-embedded heart. *Bar* represents 30 μm

NIH-PA Author Manuscript
NIH-PA Author Manuscript
NIH-PA Author Manuscript

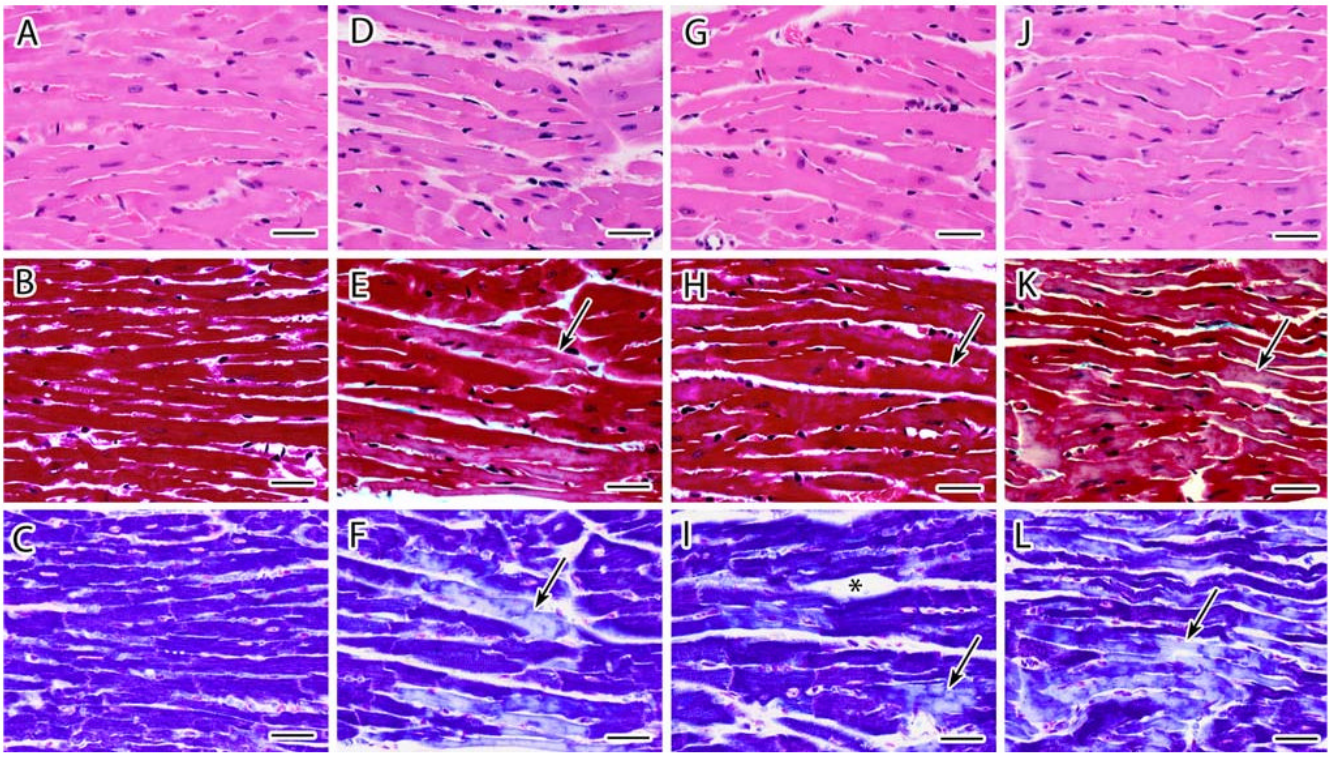

Fig. 2.

a–l Representative light photomicrographs of cardiac tissue sections stained with H&E (*top panel*), Masson's Trichrome (*center panel*), and PTAH (*lower panel*) from female CD-1 mice necropsied at 26 week of age following transplacental exposure to vehicle (**a, b, c**), 3TC (**d, e, f**), AZT (**g, h, i**) or AZT/3TC (**j, k, l**) on days 12–18 of gestation. Heart sections from vehicle-exposed mice demonstrate characteristic features of cardiomyocytes with H&E (**a**) and uniform dark staining of myofibrils with trichrome and PTAH and (**b, c**). Trichrome (**e, h, k**) and PTAH (**f, i, l**) stained cardiomyocytes in hearts from NRTI-exposed mice had areas of pale or mottled muscle fibers (*black arrows*), loss of distinct fibers and cross-striations (*black arrows*), attenuation of muscle fibers (**k, l**), and increased endomysial space (*asterisks*). The magnitude of damage appeared less than that seen at 13 weeks after in utero NRTI exposure (Fig. 2). Photomicrographs from each group represent parallel sections from the same animal. *Bar* represents 30 μm

NIH-PA Author Manuscript

NIH-PA Author Manuscript

NIH-PA Author Manuscript

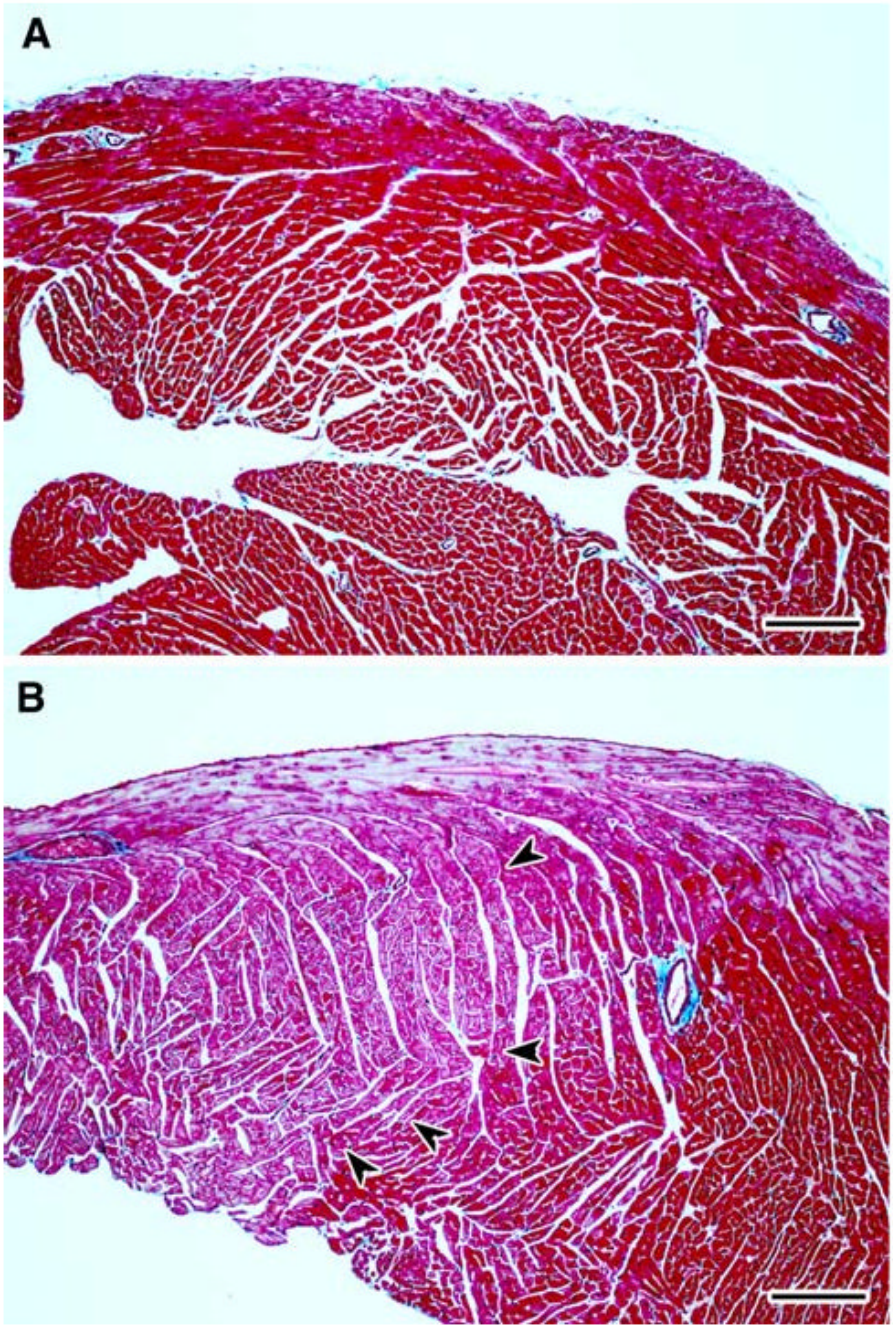

Fig. 3.

a–b Representative light photomicrographs of right ventricular free wall from cardiac tissue sections stained with Masson's trichrome from female CD-1 mice necropsied at 13 week of age following transplacental exposure to vehicle (**a**) or AZT/3TC (**b**). **a** shows uniform normochromic (*dark red*) trichrome staining in the right ventricle of a heart from a control mouse, while **b** has areas of apparent normochromic staining juxtaposed to areas of uniform pallor (*orchid color*) in the right ventricle of a heart from a mouse exposed in utero to AZT/3TC. In **b**, a line of demarcation between hypochromic areas (*left*) and normochromic areas (*right*) of cardiomyocytes is indicated by *arrowheads*. The light blue staining pattern at the top

of the right ventricle in **b** is a result of the presence of subepicardial Purkinje fibers. *Bar* represents 150 μm

NIH-PA Author Manuscript
NIH-PA Author Manuscript
NIH-PA Author Manuscript

NIH-PA Author Manuscript
NIH-PA Author Manuscript
NIH-PA Author Manuscript

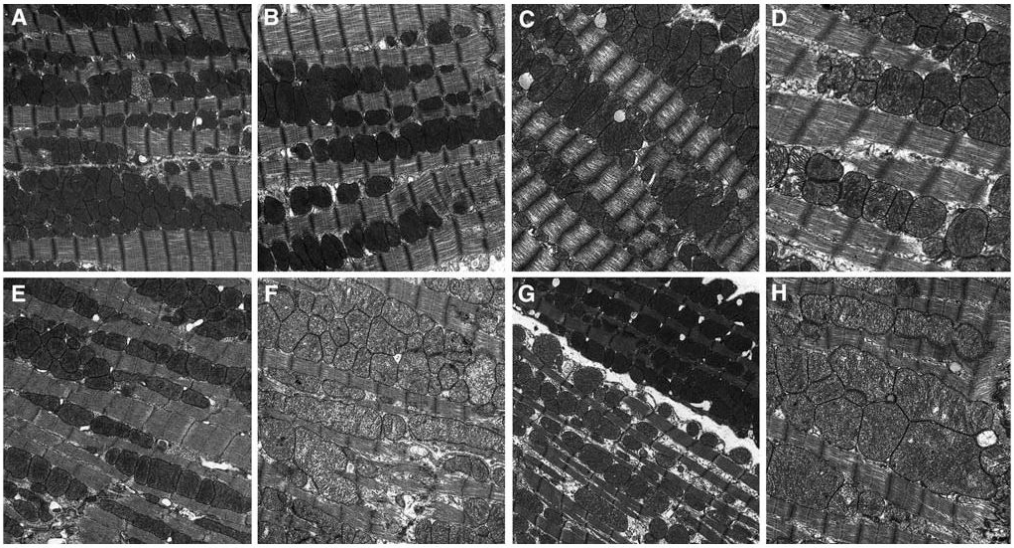

Fig. 4.

a–h Representative transmission electron micrographs from female CD-1 mice necropsied at 13 week of age following transplacental exposure to vehicle, AZT, 3TC, or AZT/3TC on days 12–18 of gestation. **a** (15,000×): vehicle-exposed control mouse cardiac muscle; mitochondria have representative size, cristae numbers, and density of matrices, are located between organized muscle fibers bundles; sarcomeres have discrete Z-bands and M-lines; a rare mitochondrion has reduced cristae numbers; **b** (20,000×): representative control mouse mitochondria and myofibrils. **c, d** 3TC-exposed mouse cardiac muscle; **c** (15,000×): enlarged mitochondria have reduced cristae numbers and disorganized myofilaments with reduced density; **d** (30,000×): mitochondria have reduced matrix density and cristae numbers; sarcomeres have reduced myofilament and Z-line density. **e, f** (20,000×): AZT-exposed mouse cardiac muscle; **e**: mitochondria have reduced numbers and fewer cristae; **f**: enlarged mitochondria have reduced matrix density, reduced cristae numbers, increased matrix granularity; sarcomeres have reduced myofilament and Z-line density. **g, h**: AZT/3TC-exposed mouse cardiac muscle. **g** (15,000×): two cells with different mitochondrial populations; uppermost cell: mitochondria have representative characteristics of controls; lower cell: mitochondria have reduced numbers, matrix density; sarcoplasm is increased with increased granularity; **h** (20,000×): enlarged mitochondria have reduced cristae numbers, sarcomeres have reduced myofilament and Z-line density, increased myofilament disorganization

NIH-PA Author Manuscript
NIH-PA Author Manuscript
NIH-PA Author Manuscript

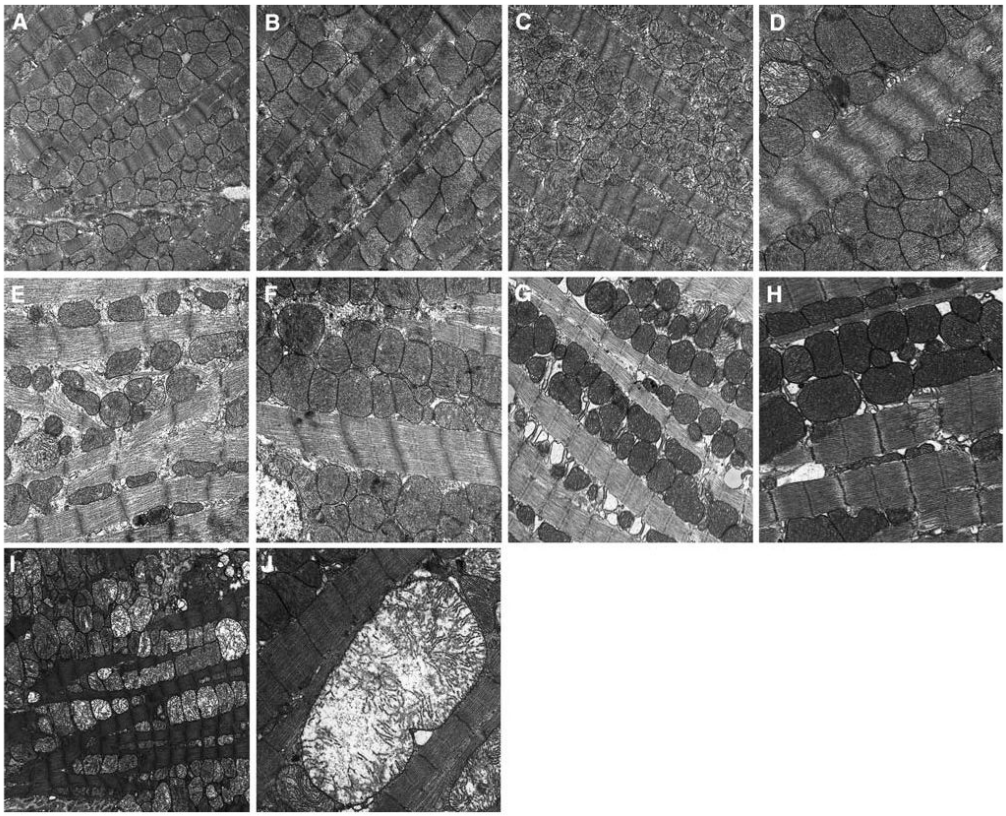

Fig. 5.

a–j Representative transmission electron micrographs from female CD-1 mice necropsied at 26 week of age following transplacental exposure to vehicle, AZT, 3TC or AZT/3TC on days 12–18 of gestation. **a** (20,000×): Control mouse cardiac muscle; mitochondria have representative sizes, cristae numbers, matrix density; **b** (25,000×): representative clusters of enlarged mitochondria seen occasionally in control mouse cardiac muscle. **c, d** 3TC-exposed mouse cardiac muscle; **c** (20,000×): increased numbers of mitochondria with reduced cristae numbers, increased metrical granularity; **d** (30,000×): enlarged mitochondria with reduced matrix density, cristae numbers, a few mitochondria have marked reduction in cristae numbers; sarcomeres have markedly reduced myofilament and Z-line density and increased myofilament and Z-line disorganization. **e, f** (30,000×): AZT-exposed mouse cardiac muscle. **e** mitochondria have reduced numbers, marked size variation, reduced matrix density and cristae numbers; sarcoplasm is increased with increased granularity; sarcomeres have markedly reduced myofilament and Z-line density and increased myofilament and Z-line disorganization; **f** enlarged mitochondria have moderate loss of matrix density; sarcomeres have reduced myofilament and Z-line density. **g, j** AZT/3TC-exposed mouse cardiac muscle; **g** (30,000×): mitochondria have increased matrix density, cristae have increased density; sarcomeres have reduced myofilament and Z-line density; **h** (30,000×) enlarged mitochondria have dense matrices and cristae; sarcomeres have multi-focal areas of disorganization of myofilaments and Z-lines; **i** (15,000×): mitochondria have markedly reduced cristae numbers, increased metrical granularity; **j** (30,000×): a single markedly enlarged mitochondrion with markedly reduced cristae numbers and a length equivalent to approximately five sarcomeres; sarcomeres have multifocal disorganization of Z-lines

NIH-PA Author Manuscript

NIH-PA Author Manuscript

NIH-PA Author Manuscript

Table 1

Semi-quantitative light microscopic analysis of heart sections from 13- or 26-week-old female CD-1 mice exposed transplacentally to 3TC, AZT, or AZT/3TC

Treatment group	Group sizes	Mean score ± SE at 13 weeks	Mean score ± SE at 26 weeks	Comparisons of values at 13- versus 26-weeks-of-age (*P*-value)
Control	$n = 4$	0.25 ± 0.39	0 ± 0	$P > 0.05$
3TC	$n = 4$	3.00 ± 0.39	1.25 ± 0.39	$P < 0.01$*
AZT	$n = 8$	2.38 ± 0.29	1.38 ± 0.28	$P = 0.01$*
AZT/3TC	$n = 8$	3.50 ± 0.28	2.25 ± 0.28	$P < 0.01$*
Comparisons of NRTI treatment groups versus controls (*P*-value)		3TC, $P < 0.001$*	3TC, $P = 0.039$*	
		AZT, $P < 0.001$*	AZT, $P = 0.01$*	
		AZT/3TC, $P < 0.001$*	AZT/3TC, $P < 0.001$*	
Comparisons of individual NRTI treatment groups (*P*-value)		3TC vs AZT, $P = 0.05$	3TC vs AZT,	
		3TC vs AZT/3TC, $P > 0.05$	$P > 0.05$ 3TC vs AZT/3TC,	
		AZT vs AZT/3TC, $P = 0.011$*	$P = 0.013$* AZT vs AZT/3TC,	
			$P = 0.017$*	

Ten-micrometer heart sections were stained with Masson's trichrome, a section from each mouse (number of mice listed in table, number of litters examined: vehicle = 4, 3TC = 3, AZT = 6, AZT/3TC = 5) was scored based upon the percentage of cardiomyocytes affected, and the values were averaged across the group to get an average ± standard error. The semi-quantitative scoring scheme was as follows: (0), within normal limits, ≤5% of cells affected; (1+) mild, 6–20% of cells affected, (2+) moderate, 21–50% of cells affected, (3+), marked, 51–80% of cells affected; (4+) severe, >80% of cells affected. *P*-values for comparison of differences among the exposure groups were obtained using a two-way ANOVA with a Holm-Sidak post hoc test. The treatment-related data from 13- and 26-week-old mice were significantly different ($P = 0.05$)

* Significant *P*-values

NIH-PA Author Manuscript

NIH-PA Author Manuscript

NIH-PA Author Manuscript

Table 2

Semi-quantitative analysis of transmission electron micrographs of hearts from 13- or 26-week-old female CD-1 mice exposed transplacentally to 3TC, AZT, or AZT/3TC

Treatment group	Group sizes	Mean score ± SE at 13 weeks	Mean score ± SE at 26 weeks	Comparisons of values at 13-versus 26-weeks-of-age (*P*-value)
Control	$n = 4$	0.21 ± 0.11	0.21 ± 0.11	$P > 0.05$
3TC	$n = 4$	1.18 ± 0.12	1.39 ± 0.14	$P > 0.05$
AZT	$n = 8$	1.18 ± 0.18	1.50 ± 0.17	$P > 0.05$
AZT/3TC	$n = 8$	1.86 ± 0.26	2.34 ± 0.24	$P < 0.05$*
Comparisons of NRTI treatment groups versus controls (*P*-value)		3TC, $P = 0.004$*	3TC, $P < 0.001$*	
		AZT, $P < 0.001$*	AZT, $P < 0.001$*	
		AZT/3TC, $P < 0.001$*	AZT/3TC, $P < 0.001$*	
Comparisons of individual NRTI treatment groups (*P*-value)		3TC vs AZT, $P > 0.05$ 3TC vs AZT/3TC, $P = 0.021$*	3TC vs AZT, $P > 0.05$ 3TC vs AZT/3TC, $P < 0.001$*	
		AZT vs AZT/3TC, $P = 0.015$*	AZT vs AZT/3TC, $P = 0.002$*	

Photomicrographs from each mouse (number of mice/litters examined: vehicle = 6 mice/4 of 6 l, 3TC = 6 mice/3 of 3 l, AZT = 7 mice/5 of 6 l AZT/3TC = 10 mice/5 of 5 l) were scored, and an average was calculated for all micrographs from each individual animal; these values were then averaged across the group to get an average ± standard error. The semi-quantitative scoring scheme was as follows: (0) within normal limits, nearly all mitochondria present had typical round or oblong shape and dense matrices containing closely packed, dark staining, and intact cristae that were situated between intact myofibrils organized into evident sarcomeres with apparent Z-discs and M-lines. (1+) mild, most mitochondria were typical in shape and numbers of cristae, occasionally a minimally swollen mitochondrion with apparent reduction in prominent cristae was identified, and alterations of myofibrils or sarcomeres were not evident. (2+) moderate, the number of mitochondria per cell was either nearly doubled or significantly reduced compared to samples scored (0) or (1+), many mitochondria were enlarged with some reduction in the number of prominent cristae and breaks in myofibrils and indiscernible sacromere Z-discs were evident in several areas. (3+) marked, clusters of highly damaged mitochondria within a cell that were abnormal in size, shape, and concentration of cristae were found, damage of myofibrils and sarcomere architecture was apparent, and occasionally a giant mitochondria containing little to no cristae or central architecture was found. (4+) severe, all or almost all mitochondria were atypical in the field of view and there was a lack of organization within muscle bundles with widespread muscle fiber damage and sarcomere disorganization. *P*-values for differences between the average values for individual animals in each NRTI-exposure group versus vehicle-exposed animals were obtained using a two-way ANOVA with a Holm-Sidak post hoc test

* Significant *P*-values